I. RADIATION AND BACKGROUNDS

A. Conventional Radiation

The proton source generates a 4-7 MW proton beam: comparable to proposed spallation sources. This is a very high power and will, as in the spallation sources, require great care in reducing unwanted particle losses, and require careful machine shielding, and target and beam dump design. Initial studies of the target and capture solenoid region have been performed with the MARS code, and preliminary specifications for shielding determined, but more work is needed.

The cooling and accelerator chain is rather clean: a relatively small fraction of the muons decay, and their energies are low. Power deposited in the accelerators is (see tables **??**, **??**, and **??**) are typically only about 10 W/m.

If no muons are lost, then the only sources of radiation are the muon decays yielding electrons and neutrinos. The neutrino radiation we discuss below. The electrons shower in the collider beam pipe shields, depositing most of their energy in the shield a nd a relatively small amount in the magnet coils and yoke. For a 4 TeV example, The MARS code [1] calculated doses after five years operation, immediately after turn off, and 1 day after turn off, are as given in table I. It is seen that the areas in the tunnel, but outside the magnets are relatively free of radioactivation. Special procedures will be needed when the shield pipe has to be opened, as for instance when a magnet is changed. For the lower energy colliders, the radioactivation levels are proportionally less.

TABLE I. Collider ring radioactivation levels (mrem/hour) after turn off.

	immediate	after 1 day
Inside face of shield	9000	4000
Outside face of shield	200	170
Outside of Coils	30	14
Outside of Yoke	3	1.4

If muons are lost: accidentally, by scraping, or deliberately after some number of turns, then the muons penetrate to considerable distances (3.5 km at 2 TeV, 800 m at 250 GeV) and deposit their energy primarily near the end of their paths. Figures 1 and 2 show the distribution of radiation levels assuming 25 % of all muons (4 bunches of 2×10^{12} at 15 Hz) are dumped into soil/rock with density 2.24 g/cm^3. It is seen that the radiation is contained within cylinders of radius $\approx$ 15 m. If any water were present in the soil/rock then the first two meters around the aborted beam axis would require insulation or drainage up to a distance of 2.5 km at 2 TeV or 550 m at 250 GeV.

B. Neutrino Radiation

It had been noticed [2] that the neutrinos created in muon beam decays can generate excessive secondary radiation at large distances from a muon collider (see Fig. 3). The surface radiation dose $D_B(Sv)$ over a time $t(s)$, in the plane of a bending magnet of field B(T), in a circular collider with beam energy $E(TeV)$, average bending field $< B(T) >$, at a depth $d(m)$ (assuming a spherical earth), with muon current (of each sign) of I(muons/s/sign) is given by:

$$D_B \;\approx\; 4.4 \times 10^{-24}\, \frac{I_\mu\ E^3\ t}{d}\, \frac{< B >}{B}\ t,$$

and the dose D_S at a location on the surface, in line with a high beta straight section of length ℓ is:

$$D_S \;\approx\; 6.7 \times 10^{-24}\, \frac{I_\mu\ E^3\ t}{d}\ \ell < B > t.$$

The later equation assumes that the average divergence angles satisfy the condition: $\sigma_\theta << \frac{1}{\gamma}$. This condition is not satisfied in the straight sections approaching the IP, and these regions, despite their length, do not contribute a significant dose. These expressions have been confirmed, and refined, by Monte Carlo simulations [3] using the MARS code. For the 3 TeV parameters given in Tb. **??** (muon currents $I = 6 \times 10^{20}\ \mu^-/yr$, $< B >= 6T$, $B = 10T$, and taking the federal limit on off site radiation Dose/year, D_{Fed} to be 1 mSv/year (100 mrem/year), then the dose D_B per year (defined as 10^7 s), in the plane of a bending dipole is:

$$D_B = 1.07 \times 10^{-5}\ \ \mathrm{Sv}\ \ \approx 1\%\ D_{Fed},$$

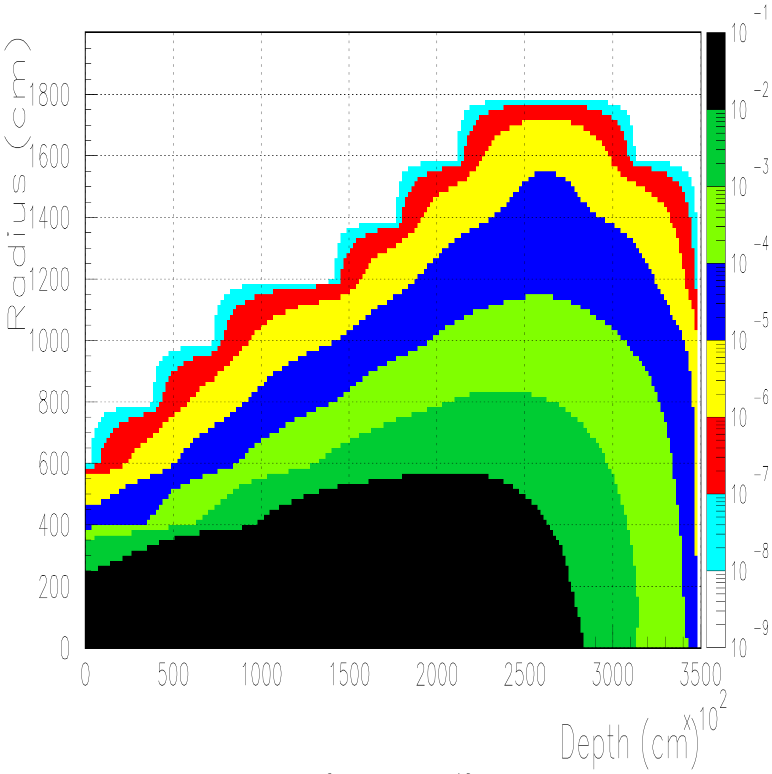

FIG. 1. Isodose contours in the soil/rock (ρ=2.24 g/cm^3) for 3×10^{13} extracted 2 TeV muons per second. Right scale is dose rate in rem/s.

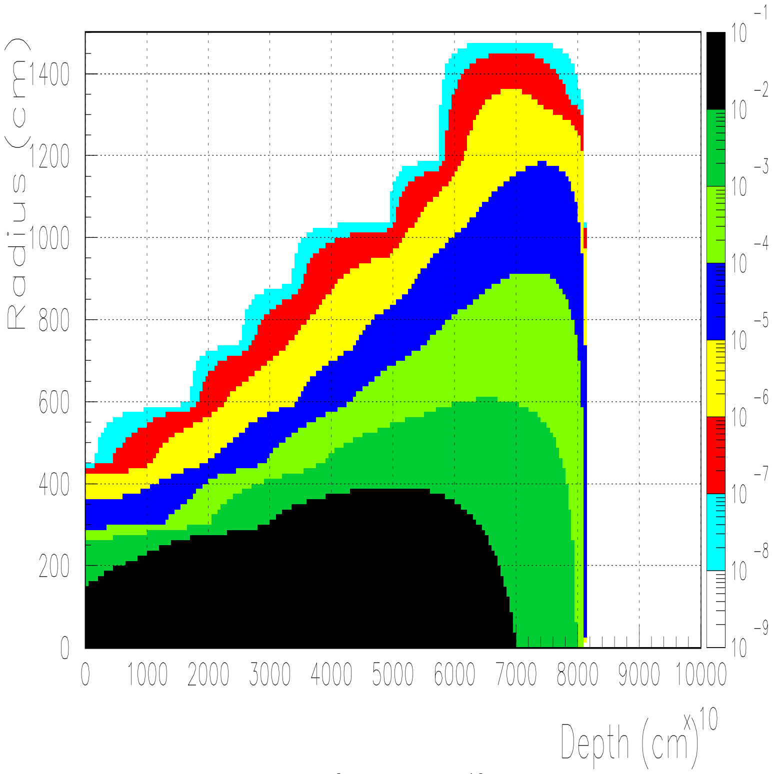

FIG. 2. Isodose contours in the soil/rock (ρ=2.24 g/cm^3) for 3×10^{13} extracted 250 GeV muons per second. Right scale is dose rate in rem/s.

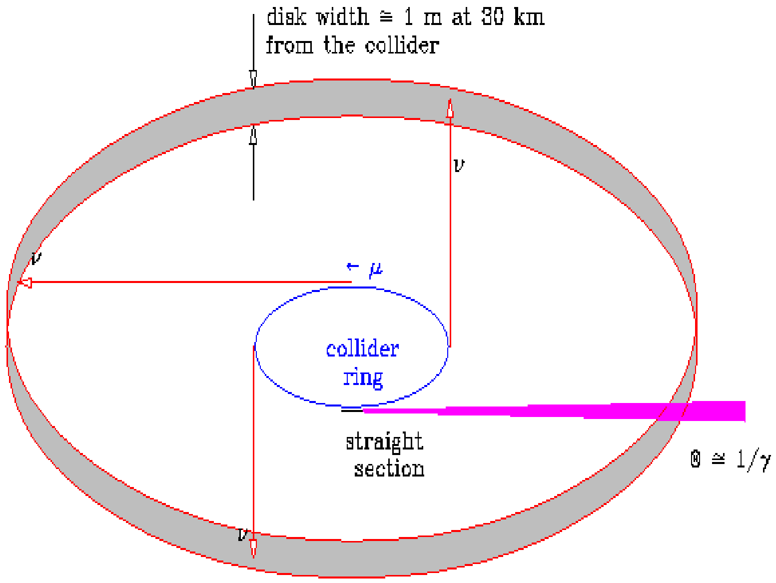

FIG. 3. Neutrino radiation disk. For a 3 TeV CoM collider the neutrino radiation width is ≈ 1 m at a distance of 30 km. A *hot spot* produced by 0.1 m straight section in the ring contains twice the number of neutrinos on the disk on average.

and for a straight section of length 0.6 m is:

$$D_S = 9.7 \times 10^{-5} \;\; \mathrm{Sv} \;\; \approx 10\% \; D_{Fed},$$

which may be taken to be within a reasonable limit.

Special design will be required in the lattice design to assure that no field free region longer 0.6 m is present. This may sound difficult, but it may be noted that the presence of a field of even 1 T, over any length, is enough to reduce the dose to the same level, and the application of such a field over all rf and other components seems practicable [3,4].

For lower energy machines, the requirements get rapidly easier: a 0.5 TeV machine at 500 m depth could have 130 m straight sections, or if at 100 m depth 25 m lengths, for the same surface dose. For a 100 GeV machine the doses are negligible.

For machines above 3 TeV, various strategies can be employed:

- The machines could be built at greater depths (mines many km deep are common).
- The vertical beam orbits in the machine could be varied so as to spread the plane of radiation and thus reduce the peak doses.
- The specific locations in line with straight sections could be purchased and restricted.
- Straight sections could be further reduced by using continuous combined function magnets. The machines could be built on an island. This would be particularly attractive since the radiation above water is intrinsically less (because of the lower water density), as well as being unoccupied for significant times.

But for any large increase in energy, to 10 TeV, for instance, some reduction in muon beam flux will probably be required. The resultant loss of luminosity might be made up in a number of ways:

- The beam-beam tune shift constraint could be avoided by introducing a conducting medium (e.g. liquid lithium) at the interaction point [5].
- The focusing strength could be increased by the use of plasma or other exotic focusing method.
- Better cooling could be developed. Optical Stochastic Cooling [6], for instance, might reduce the emittances by many orders of magnitude, thus greatly reducing the required beam currents. Indeed, such cooling would require lower currents to function appropriated.

Such options will need future study.

C. Muon Decay Background

With 4×10^{12} muons per bunch in the collider ring there are approximately 4×10^5 muon decays per meter giving rise to high energy electrons. These off-energy, off-axis electrons undergo bremsstrahlung when they traverse magnetic fields and when exiting the beam pipe interact and produce electromagnetic showers and to a lesser extend hadrons and muons. Much of this debris can be locally shielded so the primary concern is muon decays near the Intersection Point (IP) [7]. This is th e background we discuss in some details below.

Figure 4 shows the final 130 meters which include the final four quadrupoles, dipoles and a solenoidal field surrounding the detector. Detailed Monte Carlo simulations of electromagnetic, hadronic and muon components of the

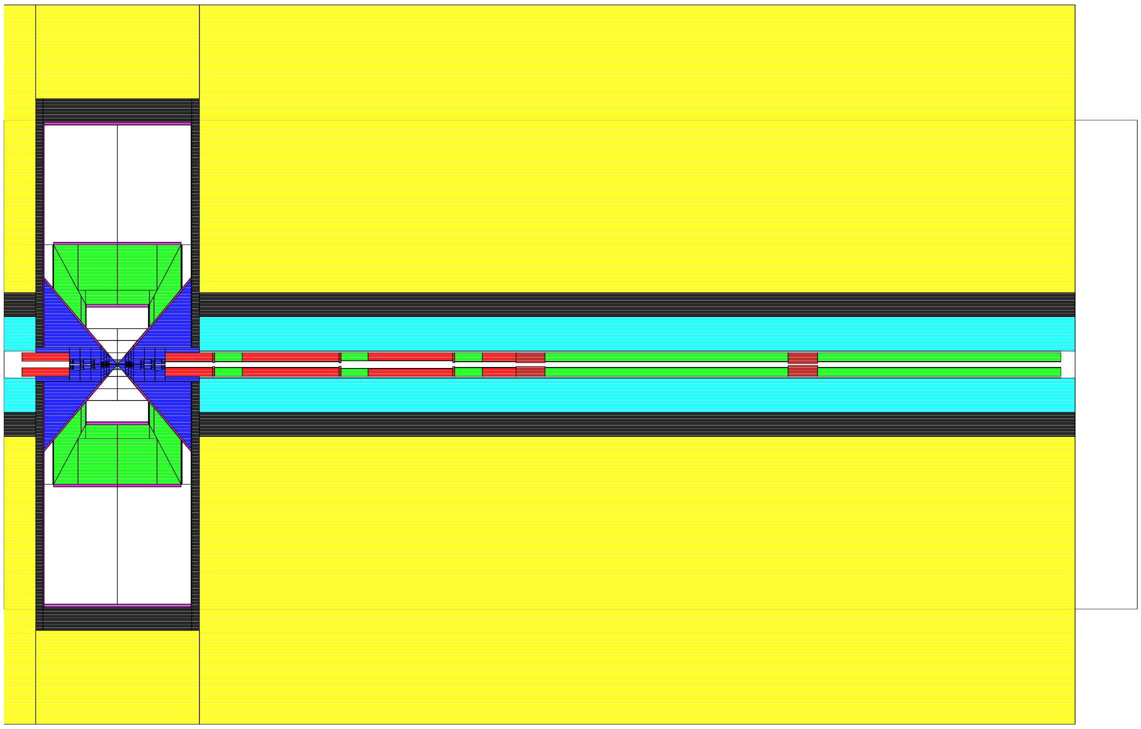

FIG. 4. Region around the Intersection region modeled in GEANT. The triangular blue regions represent tungsten shielding. On the right side of the figure, the red areas represent quadrupoles in the beam line. The areas around the IP represent the various detector volumes used in the calculations of particle fluences.

background [7–10,4,11,12] have been performed using the MARS [13] and GEANT [14] codes. The most recent study [11] has been done with GEANT.

This study:

- followed shower neutrons and photons down to 40 keV and electrons to 25 keV.
- used a tungsten shield over the beam, extending in to within 14 cm of the intersection point, and extending outward to an angle of 20 degrees from the axis.
- inside this shield, between its smallest aperture 1 m from the IP, and its tip, the inner surface is shaped into a series of rising collimating steps and slopes, designed so that, the detector could not *see* any surface directly illuminated by the initial decay electrons, whether in the forward or backward (albedo) directions (see figure 5).
- from the aperture point of minimum radius to a few meters (2.5 m for Higgs Factory) upstream, the inside forms another series of stepped collimators placed at $\pm$ 4 σ_{θ_0} (where σ_{θ_0} is the rms divergence of the beam).
- further upstream, prior to the first quadrupole (from 2.5 to 4 m in the Higgs case) an 8 T dipole, with collimators inside, is used to sweep decay electrons before the final collimation.

Every modern detector will have to be able to identify and reconstruct secondary vertices such as b's. In order to estimate the viability of a vertex detector we have to show that the occupancy of its elements is not higher than about

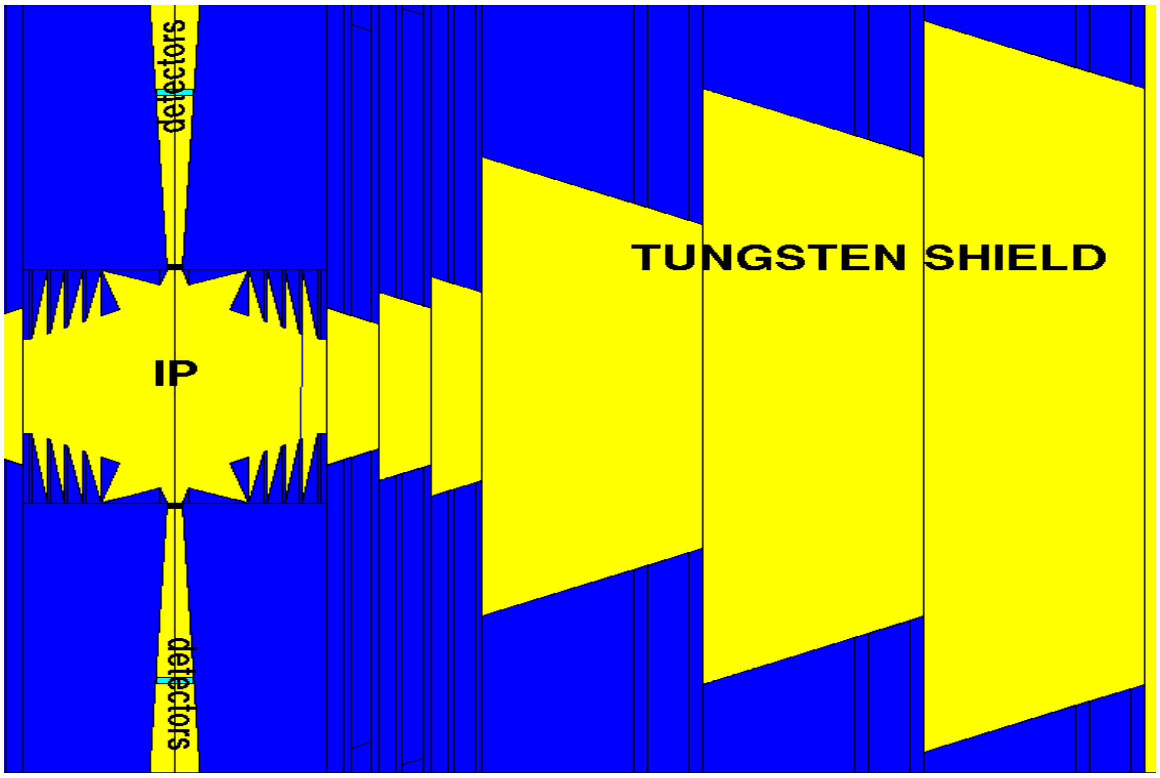

FIG. 5. Detail of the tungsten shielding designed so that the detector is not connected with an straight line with any surface hit by decay electrons in both forward or backward direction.

1 %. Figure 6 shows the occupancy as a function of radial distance from the Intersection Point for the three energies studied : 50×50, 250×250 GeV and 2×2 TeV . The occupancy was calculated for silicon pads of 300×300 μm. One can observe that the total occupancy (left figure) is above one percent for small radii . The majority of the hits are due to conversions of photons. Since the average energy of the background photons is only 1 MeV, then if one uses a pairs of silicon detectors inter-spaced by about 1 cm, the electrons resulting from photon conversions will curl in the 4 T solenoidal field and will never trigger the second member of the paired detectors. A simple coincidence requirement would eliminate most of the hits induced by neutral particles. The remaining charged occupancy is below 1% (right figure). One can also lower the occupancy at small radii by using smaller pixel sizes, as, for instance, indicated in table II below.

Table II gives the hit density for the Higgs factory from the various sources and the occupancy of pixels of the given sizes. In all cases the numbers are given per bunch crossing. The hit density for the higher energy machines is found to be somewhat lower than these, due to the smaller decay angles of the electrons.

TABLE II. Detector backgrounds from μ decay

Radius	cm	5	10	20	100
Photons hits	cm^{-2}	26	6.6	1.6	0.06
Neutrons hits	cm^{-2}	0.06	0.08	0.2	0.04
Charged hits	cm^{-2}	8	1.2	0.2	0.01
Total hits	cm^{-2}	34	8	2	0.12
Pixel size	μm^2	60x150	60x150	300x300	300x300
Occupancy all	%	0.6	0.14	0.4	0.02
Occupancy charged	%	0.14	0.02	0.04	0.002

The radiation damage by the neutrons on a silicon detector has also been estimated. In the Higgs case, at 5 cm from the vertex, the number of hits from neutrons above 100 keV is found to be 1.8×10^{13} per year (10^7 s). This is significantly less than that expected at the LHC (LHC is now ordering silicon detectors claimed to have a life

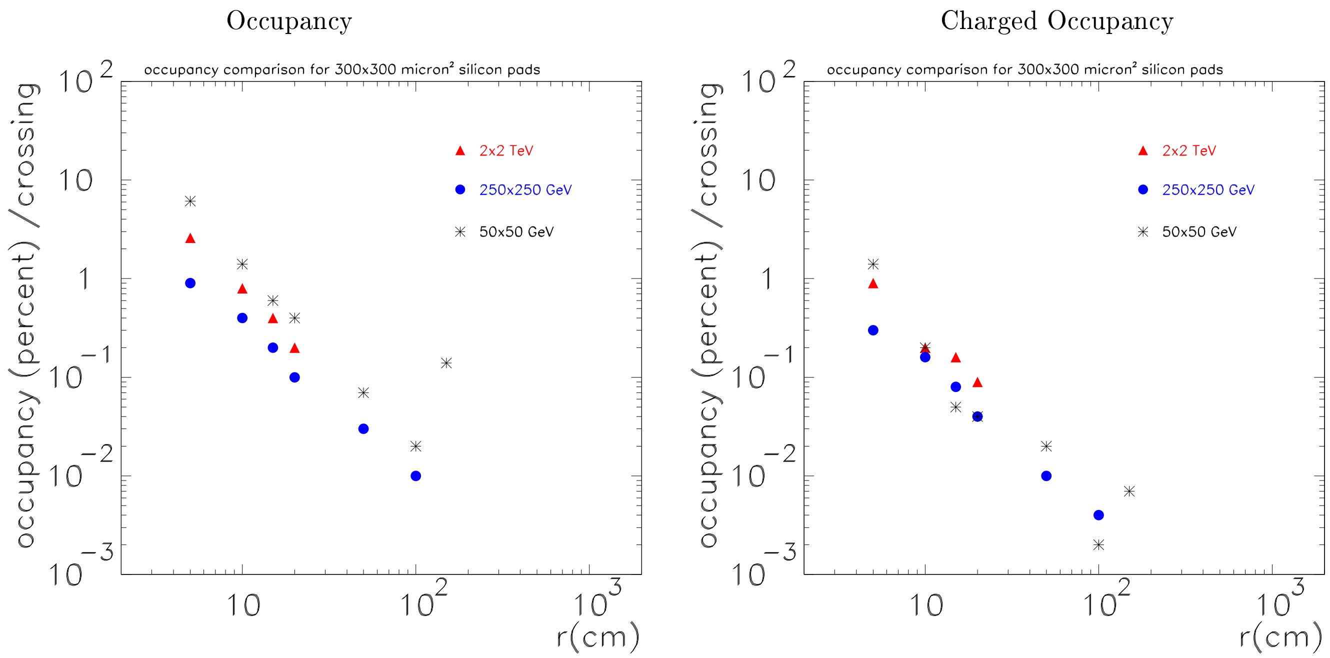

FIG. 6. Occupancy as a function of the radius for the three energies studied. Left figure shows the total occupancy and right the charged occupancy.

expectancy of 5×10^{14}, approximately three times that assumed here). The damage for silicon detectors in the higher energy machines is of the same order (see Table III).

TABLE III. Radiation damage by neutrons on silicon detectors. The working assumptions are: 1000 turns, 15 Hz and 1 year=10^7 s. An acceptable number of hits per year is 1.5×10^{14}.

CoM	μ's/bunch	neutrons/cm^2/crossing	Hits/year	Lifetime
TeV	10^{12}	above 100 KeV	10^{13}	years
4	2	100	3	5
0.5	4	50	3	5
0.1	4	30	1.8	8

This study also found a significant flux of muons, with quite high energies, from μ pair production in electromagnetic showers (Bethe-Heitler). Their most serious effect appears to arise when they make deeply inelastic interactions and deposit spikes of energy in the electromagnetic and hadronic calorimeters. This is not serious in the Higgs case, for which the fluxes and cross sections are low, but at higher energies timing and/or longitudinal calorimeter segmentation appears necessary to identify and remove the problem.

Earlier studies with code MARS, using less sophisticated shielding, gave results qualitatively in agreement with those from Geant.

D. Halo Background

Muon halo refers to those muons which are lost from the beam bunch as it circulates around the collider ring. In conventional electron or proton accelerators, beam particles which are lost away from the IP are of little concern as they can be locally shielded. However, muons can traverse long distances and therefore, have the potential to generate background in a detector. The magnitude of this background depends on a detailed knowledge of the injected beam profile and a credible model for beam halo and beam losses. More work is needed before these are well enough understood.

The beam will need careful preparation before injection into the collider, and the injection system will have to be precise and free of ripple. The collimation system described above was designed to scrape the beam both initially and during the 1000 turns, to assure that all loss occurs at the scraper and not near the IP. That study indicated a suppressions by better than 10^3 of background in the detector due to these scrapers. The use of magnetized iron deflectors can probably further reduce this.

Beam loss must be limited as far as possible. Gas scattering has been studied [15] and shown to give a negligible contribution. The effects of beam-beam scattering are under study and need further work. Momentum spread tails from uncorrected wake field effects must be controlled. Assuming that the total loss from all causes, after injection and the first few turns is less than 10^{-4} in 1000 turns, (i.e. 10^{-7} per turn), then the number of background muons passing through the detector should be less than 800 ($2 \times 4 \times 10^{12} \times 10^{-3}$/[1000 turns]). This is a low density of tracks per cm^2 and should be acceptable, but lower losses or better scraping would be desirable.

E. Pair Production

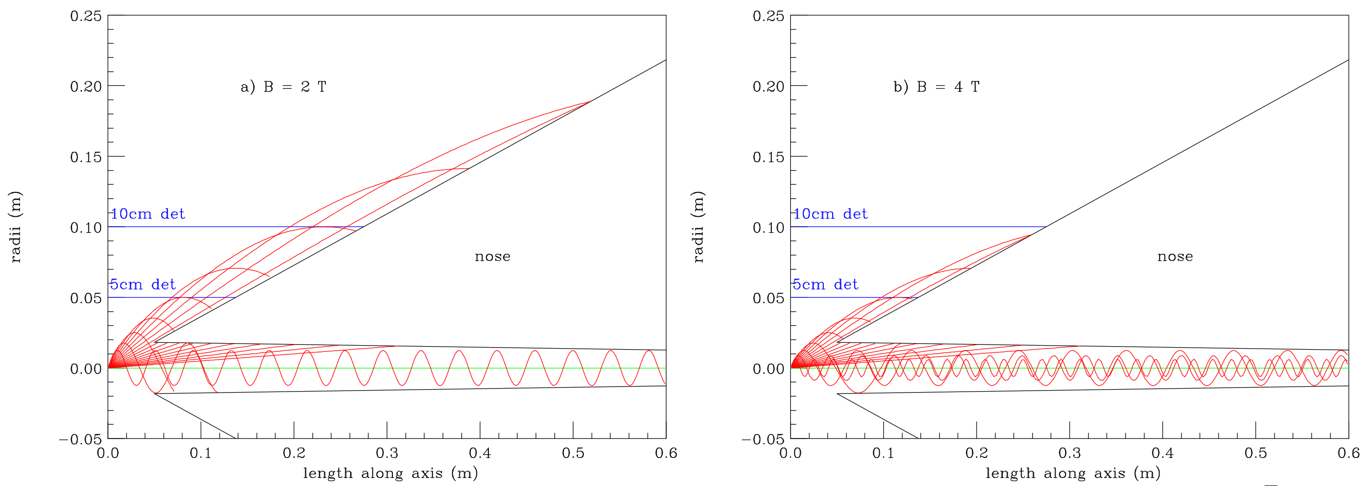

FIG. 7. Radius vs. length of electron pair tracks for initial momenta from 3.8 to 3000 MeV in geometric steps of $\sqrt{2}$; (a) for a solenoid field of 2 T, (b) for 4 T.

Coherent beam-beam electron pair production (beamstrahlung), despite an early worry, has been shown [16,17] to be negligible, but the incoherent pair production (i.e. $\mu^+\mu^- \to e^+e^-$) pair production in the 4 TeV collider case at high energies is significant.

The cross section is estimated to be 10 mb [17], which would give rise to a background of $\approx 3 \times 10^4$ electron pairs per bunch crossing. The electrons at production, do not have significant transverse momentum, but the fields of the oncoming 3 μm bunch can deflect them towards the detector. A simple program was written to track electrons from close to the axis (the worst case) as they are deflected away from the bunch center. Once clear of the opposing bunch, the tracks spiral under the influence of the experimental solenoid field. Figures 7 shows the radii vs. length of these electron tracks for initial momenta from 3.8 to 3000 MeV in geometric steps of $\sqrt{2}$ and a solenoid field of 2 T, see Fig.7a (Fig. 7(b) it is 4 T). In the 2 T case, tracks with initial energy below 30 MeV do not make it out to a detector at 10 cm, while those above 100 MeV have too small an initial angle and remain within the shield. Approximately 10 % (3000) of these are in this energy range and pass through a detector at 10 cm. The track fluence at the ends of the detector are less than 10 tracks per cm^2 which should not present a serious problem. At 5 cm, there are 4500 tracks giving a fluence of 30 per cm^2, which is also probably acceptable. If the detector solenoid field is raised to 4 T then no electrons reach 10 cm and the flux at 5 cm is reduced by a factor of 2.

F. Bethe-Heitler Muons

This study also found a significant flux of muons, with quite high energies, from μ pair production in electromagnetic showers (Bethe-Heitler). Figures 8(a) and (b) show the trajectories of typical muons from their sources in the shielding around the beam pipe to the detector. Figure 8(a) is for a 2 + 2 TeV collider, where the muons have high energy and long path lengths. A relatively long (130 m) section of beam pipe prior to the detector is shown. Figure 8(b) is for the 50 + 50 GeV collider for which, since the muons have rather short path lengths, only a limited length of beam pipe is shown. Note that the scales are extremely distorted : the 20^o shielding cones on the right hand side of the figures appear at much steeper angles.

TABLE IV. Bethe Heitler Muons

CoM Collider Energy (TeV)	4	0.5	0.1
Assumed source length (m)	130	33	20
μ ($p_{muon} > 1\ GeV/c$) per electron	$5.4\ 10^{-4}$	$8.3\ 10^{-5}$	$9.6\ 10^{-6}$
Beam μ's per bunch	$2\ 10^{12}$	$2\ 10^{12}$	$4\ 10^{12}$
B.H. μ's per bunch crossing ($\times 10^3$)	28	17.5	6.1
$< p_{muon} >$ initial (GeV)	22	9.5	4.4
μ's entering calorimeter	220	160	25
$< p_{muon} >$ (GeV)	15.4	6.3	1.8
$< E_{dep} >$ (GeV)	2.9	1.3	0.4
Total E_{dep} (GeV)	640	210	10
E_{dep} pedestal subtracted (GeV)	50	25	1
Fluctuation in E_{dep} (GeV)	55	15	1
E_{trans} pedestal subtracted (GeV)	15	15	.5
Fluctuation in E_{trans} (GeV)	40	8	0.5

FIG. 8. trajectories of typical Bethe Heitler muons from their sources in the shielding around the beam pipe to the detector. a) for a 2 + 2 TeV collider, b) for 250 + 250 GeV Collider.

Their most serious effect appears to arise when they make deeply inelastic interactions and deposit spikes of energy in the electromagnetic and hadronic calorimeters. This is not serious in the Higgs case, for which the fluxes and cross sections are low, but at the higher energies they generate significant fluctuations in global parameters such as transverse energy and missing transverse energy

Tb. IV gives some parameters of the muons for three different machine energies. In the 2 + 2 TeV and 250 + 250 GeV cases, massive lead shielding outside the focus quadrupoles has been included.

Figures 9(a) and (b) show energy deposition from Bethe Heitler muons in a typical bunch crossing; they are plotted against the rapidity and azimuthal angles in the calorimeter: a) for 2 + 2 TeV, b) for 250 + 250 GeV. The massive lead shielding referred to above was not included in this study. Figure 9(c) and (d) show the same distributions with a 1 ns timing cut. It is seen that the timing cut, if it is possible, is effective at removing energy spikes at small rapidity, but has little effect in the forward and backward directions. The overall reduction in energy deposition is about a factor of two.

The energy spikes can cause several problems: they effect the triggers and event selections based on overall or transverse energy balance; they can generate false jets and they can give errors in the energies of real jets. After a pedestal subtraction, the effects on energy balances do not seem serious. The generation of false jets can be eliminated by a longitudinal energy distribution cut without introducing significant inefficiency. Energy errors in real jets appears to be the most serious problem. They can be reduced by the application of radial energy distribution cuts, but such cuts introduce significant inefficiencies for lower energy jets. More study is needed.

Earlier studies [18] with code MARS, using less sophisticated shielding, gave results qualitatively in agreement with those from Geant.

[1] N. V. Mokhov, *Proceedings of the 1996 DPF/DPB Summer Study on High-Energy Physics, Snowmass'96* (Stanford Linear Accelerator Center, Menlo Park, CA), 1996.
[2] B. King, presentation at the Muon Collider Mini-Workshop: Lattice and Background, UCLA and private communication, 1997, (unpublished).
[3] N. V. Mokhov and A. Van Ginneken, Muon Collider Neutrino Radiation, presentation at the Muon Collider Collaboration Meeting, Orcas Is., Washington, 1997.
[4] C. Johnstone and N. V. Mokhov, presented at the PAC97, Vancouver, Canada (unpublished).

FIG. 9. Energy deposition from Bethe Heitler muons *vs.* the rapidity and azimuthal angles in the calorimeter: a) for 2 + 2 TeV, b) for 250 + 250 GeV. c) and d) show the same distributions with a 1 ns timing cut.

[5] A. Skrinsky, submitted to Proc. of the 4th Int. Conf. on Physics Potential and Development at $\mu^+\mu^-$ Colliders, San Francisco, CA, 1997, (to be published).
[6] A. A. Mikhailichenko and M. S. Zolotorev, Phys. Rev. Lett. **71**, 4146 (1993).
[7] Muon Collider Collaboration, in *Proceedings of the 1996 DPF/DPB Summer Study on High-Energy Physics Snowmass'96,* New Directions for High-Energy Physics (Stanford Linear Accelerator Center, Menlo Park, CA, 1997), for updated information, see the Muon Collider Collaboration WEB page at the URL, http://www.cap.bnl.gov/mumu/.
[8] C. J. Johnstone and N. V. Mokhov, *Optimization of a Muon Collider Interaction Region with Respect to Detector Backgrounds and the Heat Load to the Cryogenic Systems* , Proceedings of the 1996 DPF/DPB Summer Study on New Directions for High Energy Physics (Snowmass'96) and Fermilab-Conf-96/366, 1996., 1996.
[9] G. W. Foster and N. V. Mokhov, in *Physics Potential & Development of $\mu^+\mu^-$ Colliders 2^{nd} Workshop* (AIP Press, Woodbury, New York, YEAR).
[10] N. V. Mokhov and S. I. Striganov, *Proceedings of the 9th Advanced ICFA Beam Dynamics Workshop* (AIP Press, Woodbury, New York, 1996), Vol. 372, pp. 234–256; also Fermilab–Conf–96/011 (1996).
[11] I. Stumer et al., in *Proceedings of the 1996 DPF/DPB Summer Study on High-Energy Physics, Snowmass'96* (Stanford Linear Accelerator Center, Menlo Park, CA, 1996).
[12] N. V. Mokhov, Nucl. Phys. B **51A**, 210 (1996).
[13] N. V. Mokhov, The MARS Code System Userś Guide, Fermilab-FN-628; available at http://www-ap.fnal.gov/MARS/, 1995.
[14] *GEANT manual, v.3.2.1, CERN program Library W5013*, CERN, 1994.
[15] See [7], section 8.5.3.
[16] P. Chen, in *Proceedings of the Symposium on Physics Potential & Development of $\mu^+\mu^-$ Colliders*, Vol. 51A of *Proceedings Suppl. Nucl Phy B*, edited by D. Cline (North-Holland, The Netherland, 1996), p. 179.
[17] I. Ginzburg, in *Proceedings of the Symposium on Physics Potential & Development of $\mu^+\mu^-$ Colliders*, Vol. 51A of *Proceedings Suppl. Nucl Phy B*, edited by D. Cline (North-Holland, The Netherland, 1996), p. 186.
[18] N. V. Mokhov, Nucl. Phys. B **51A**, 210 (1996).